Materials Research. 2024; 27(suppl. 2):e20240148
DOI: https://doi.org/10.1590/1980-5373-MR-2024-0148

Synthesis of MgO Using the Sol-gel Method: Correlation Between CTAB Surfactant Concentration and MgO Properties

Gabriel R. Silva[a], Matheus S. Assis[a], João C. P. de Souza[a], Luiz G. Possato[a]*

[a]*Universidade Estadual Paulista* (UNESP)*, Faculdade de Ciências, Departamento de Química, Bauru, SP, Brasil.*

Received: April 02, 2024; Revised: June 05, 2024; Accepted: June 11, 2024

In this work, the surfactant cetyltrimethylammonium bromide (CTAB) was applied to observe how increasing the surfactant's concentration will affect the MgO characteristics, such as the increase in vacancies. The samples were characterized by X-ray diffraction (XRD). For the MgO-0.025CTAB sample, the intensity of the (200) peak of MgO decreased by three. However, the MgO-2.5CTAB showed an increase in the peaks intensity. In addition to using Rietveld refinement, it is possible to observe the textural characteristics of the samples, with the introduction of CTAB, oxygen vacancies increased, and from the MgO to the MgO-0.025CTAB sample, there was a decrease in oxygen occupancy from 94% to 82% in the unit cell. Thermogravimetry (TG) analyses were used to understand the interactions between the support and the surfactant as the CTAB concentration increased. With the physisorption of N_2, the behavior of the sample pores and specific area determination are verified. The introduction of CTAB caused the decrease of the specific area from 32 m^2/g to 9 m^2/g for the MgO and MgO-0.025CTAB samples. However, for a more concentrated surfactant, MgO-2.5CTAB, the specific area was 25 m^2/g. Scanning electron microscopy made it possible to observe the increase in the roughness with CTAB presence.

Keywords: *MgO, sol-gel synthesis, CTAB surfactant, oxygen vacancy, catalysts support.*

1. Introduction

Highly effective and low-cost catalytic materials are a significant field in the current research sector, seeking to use materials that are easy to obtain in addition to processes with low energy costs. A material capable of providing this is magnesium oxide (MgO), which, during catalysis, supports the active phase of the metal[1]. Magnesium oxide can improve the event's performance in specific reactions, such as the reforming of ethanol vapor[2], and is a molecule with high basicity, which is very important during carbon dioxide (CO_2) hydrogenation[3].

The MgO synthesis methodology is decisive in producing the material with the desired properties. Among the available description methods, the sol-gel method has gained prominence due to its effectiveness in production and being a low-cost process, as it uses little raw material and is viable on an industrial scale[4,5]. Furthermore, the possibility of adjusting the final material's properties by modifying property parameters opens the way to explore new characteristics and applications of MgO. During the description, adding a surfactant is a viable possibility to change the textural attributes of the material[6,7].

Over the years, the release of carbon dioxide into the atmosphere has become more frequent, which has led to the search for solutions to reduce the presence of CO_2[8]. Energy generation and storage are essential for the functioning of contemporary society, but using renewable energy is necessary to minimize environmental damage caused by fossil fuels. In this sense, a topic of research interest is the creation of catalytic materials suitable for converting carbon dioxide into reusable byproducts[9-11]. From the catalytic point of view, the increase in oxygen vacancies in the MgO structure is essential during its interaction with CO_2 (acid molecule). MgO is also less prone to forming oligomeric carbon species on the surface due to competitive water adsorption. Carbonaceous compounds decompose before polymerization on the catalyst surface[12]. Carbon dioxide is acidic, and there will be interaction with MgO, which has high basicity, and structural flaws promote this reaction[13-16]. Magnesium oxide, a mostly low-cost material, and an easily accessible raw material source, is present in many CO_2 methanation reactions. Its high basicity contributes to forming interesting byproducts for the production point. From an industrial perspective, in the medicinal area, another way of using its high basicity, magnesium oxide is used as an antacid, helping to control heartburn.

Sol-gel synthesis is one of the current forms of synthesis that, over time, has proven to be an excellent choice for those seeking to follow the principles of green chemistry[17]. The ability to produce materials with high purity and homogeneity at relatively low temperatures, thus generating low energy costs, in addition to allowing precise control of the composition and microstructure of the synthesized materials. These benefits make the sol-gel method ideal for manufacturing advanced materials with controlled final products. However, this method also has some disadvantages, such as the long duration of the process and the need to strictly control the synthesis conditions to avoid the formation of cracks and other imperfections in the final materials[17,18]. Magnesium oxide stands out as a

*e-mail: gustavo.possato@unesp.br

material of great importance in chemical synthesis due to its outstanding properties. This compound is highly valued for its stability, making it excellent catalyst support in reactions that cause high temperatures[19]. In addition, MgO has a high specific surface area and a crystalline structure that favors reagent adsorption, altering the reaction efficiency[20]. Its basic nature also allows the neutralization of acids during synthesis processes, contributing to the supply of purer products.

The synthesis by the sol-gel method allows the control of the characteristics of the final products, the introduction of the surfactant cetyltrimethylammonium bromide (CTAB), allows the increase of oxygen vacancies in the final products of the synthesis, a desired characteristic for reactions in the catalysis area, in addition to allowing the increase of the surface area, another important characteristic in catalysis reactions. In addition, if necessary, the synthesis can be modified by introducing other surfactants, aiming at different textural modifications, for use in other applications.

In this work, the surfactant CTAB was applied, seeking to observe how increasing the concentration of the surfactant will affect the properties of the material, such as the increase in vacancies, which are flaws in the crystalline structure, such as one that is absent in its position in the crystal lattice. The samples were characterized by X-ray diffraction (XRD), making it possible to determine how the increase in CTAB concentration influences the crystallinity of the sample. In addition to using Rietveld refinement, it was possible to observe the textural characteristics of the samples, such as vacancies, unit cell size, and crystal size. Thermogravimetry analyses (TGA) were applied to understand the interactions between the support and the surfactant as the CTAB concentration increased. With the physisorption of N_2, the behavior of the sample pores and specific area determination were verified, and the scanning electron microscopy made it possible to observe the morphology of the crystals.

2. Experimental

2.1. Synthesis MgO

The samples were prepared according to Aamir Hanif et al.[21] procedure, with modifications. 12.3 g of $Mg(NO_3)_2.6H_2O$ (Sigma Aldrich, 98%) was solubilized in 12.0 mL of stirred deionized water, and 0.1 g (0.025 mmol) of cetyltrimethylammonium bromide - CTAB - (Sigma Aldrich, 98%), then 30 g of NH_4OH solution (Synth, 27%) was added. The solution was stirred for 5 min at room temperature. The bottle was closed to prevent any gas from escaping, heated to 60 °C in a water bath, and stirred for 6 hours. Then, the bottle was opened, the heating was stopped, and it was kept under agitation for 24 h. The precipitate from the solution was separated by centrifugation, washed with distilled water, and dried for 24 h at 70 °C. The material was calcined at 650 °C for 12 h, and the calcination temperature was attained at a ramp rate of 1 °C/min. This solid obtained was named MgO-0.025CTAB. Other syntheses were prepared with CTAB surfactant: 0.25 and 2.5 mmol. The resultant samples were named MgO-0.25CTAB and MgO-2.5CTAB, respectively. A sample without CTAB, the MgO sample, was obtained for comparison.

2.2. Characterization of the MgO

The precursor resins were characterized using the TGA technique to assess thermal decomposition. Under oxidizing atmosphere, the analyses were performed using an STA 449 F3 instrument (Netzsch) in the temperature range of 30-1000 °C (10 °C/min), using 10 mg of the sample, an open α-Al_2O_3 crucible, and a dry air atmosphere (70 mL/min).

The crystalline phases in the calcined samples were analyzed by X-ray diffraction using a Rigaku DMAX Ultima+ diffractometer with Cu Kα radiation (40 kV/20 mA). Data were collected in the 2θ range from 5 to 90 °, with a scan step interval of 0.03 °. The refinement of the crystalline structure was performed using the Rietveld profile method using MAUD software[22,23]. The scale factors, zero shifts, and backgrounds of the peak profiles and the lattice parameters were refined using a sixth-degree Chebyshev polynomial. To calculate the oxygen vacancy, the occupancy factor for O atoms was refined. Pseudo-Voigt functions were employed for the peak profile refinements. Other parameters were not refined.

Using a Micromeritics ASAP 2010 physisorption system, nitrogen adsorption–desorption isotherms were measured at liquid nitrogen temperature (~77 K) in the relative pressure range of 0.002 to 0.998. Before the measurements, the samples were degassed for 12 hours at 200 °C while held at 10 µPa of vacuum. The specific surface area was determined using the Brunauer-Emmett-Teller (BET) formula[24]. The BJH method was used for the determination of the mesopore size distribution[25].

A Zeiss EVO-LS15 scanning electron microscope was used to assess the MgO overall shape. The samples were made in isopropanol suspension, placed on copper strips, and covered in gold.

3. Results and Discussion

3.1. Structural characteristics of the catalysts

The samples before calcination treatment were analyzed using TGA (Figure 1a). The MgO sample showed a mass loss of 25% at 360 ºC due to the composition of the magnesium hydroxide[26]. The DTG and DTA confirm the temperature of decomposition (Figure 1b and Figure 1c, respectively). Adding CTAB, the temperature of decomposition increased to 400 ºC for MgO-0.025CTAB and MgO-0.25CTAB.

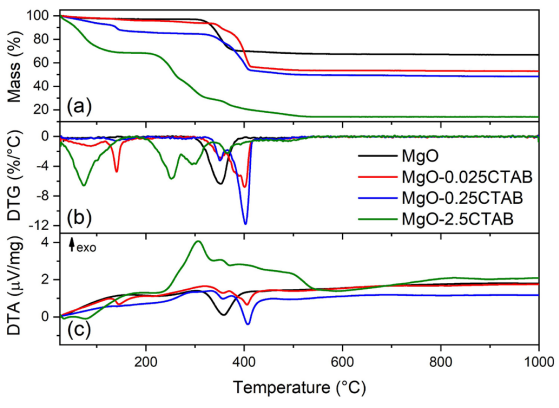

Figure 1. (a) Mass loss patterns for MgO samples, (b) DTG patterns for the MgO samples, and (c) DTA patterns for the MgO samples.

Similar to the MgO sample, the DTA and DTG profiles substantiate the occurrences at this temperature range. However, a noteworthy deviation in the MgO-0.025CTAB sample is characterized by a minor signal at 140 °C. This signal, being endothermic in nature, indicates the evaporation or elimination of water[27]. According to Mastuli et al.[27] the shift to higher temperature suggested an interaction between the magnesium species and the CTAB. The decomposition of CTAB surfactant showed a different feature (Figure S1, Supplementary Material), with the inflection point at 250 ºC. For the MgO-2.5CTAB sample, it is possible to notice that its profile for mass loss is more similar to isolated CTAB. Suggesting that the sample presents a different interaction from the others, which may be associated with the aggregation of CTAB particles and that they are encapsulating the magnesium particles[28].

The MgO sample showed X-ray diffraction peaks related to the MgO crystalline structure and an amorphous contribution (Figure 2). The standard ICSD Collection Code 26958 was used for indexing. The diffractograms showed no peaks associated with other crystalline phases, indicating that the crystalline material included solely the periclase MgO crystal structure, which has a cubic unit cell parameter of 4.22 nm[29].

The X-ray diffractograms showed a decrease in peak intensity as the CTAB introduction. For the MgO-0.025 sample, the intensity of the (200) peak of MgO decreased by three- compared to the sample prepared under similar conditions but without surfactant. Despite the considerable reduction of the crystallinity, all the peaks related to the periclase structure were detected after the synthesis. For the MgO-0.25CTAB sample, the intensities of the reflections decreased further, with the peaks related to the less intense reflections, such as (111) and (400), tending to disappear. However, for the sample with the highest concentration of CTAB MgO-2.5CTAB, the intensity of the reflections increased, indicating a break in the trend of reduction in crystallinity. This result suggests an optimum concentration at which CTAB can contribute to decreasing the crystallinity, and its excess is detrimental to the synthesis.

In the deep analysis of the crystalline structure by the Rietveld refinement method (Table 1), all samples revealed the cubic cell parameter 4.21 nm. Surfactants such as CTAB can influence the properties of colloidal systems, such as suspensions or emulsions, and may sometimes impact crystal structures[30]. However, the idea that surfactants can directly decrease the unit cell of a crystal structure is not typical behavior of surfactants[31]. The unit cell in crystallography refers to the smallest repeating unit of a crystal lattice. It is defined by the lengths of its edges and the angles between them. Surfactants, when interacting with crystals or colloidal systems, typically affect surface properties, aggregation, or dispersion of particles, but they don't directly change the fundamental parameters of the crystal lattice[28]. It's worth noting that some surfactant-like molecules can influence crystal growth and morphology. However, the effect is often more complex and depends on the specific interactions between the surfactant and the crystal surface.

The precise interactions between the surfactant molecules and the developing crystal surfaces determine how surfactants affect the crystallite size. The stability of nanoparticles, controlled nucleation and growth, surface energy modification, template or structure-directing agents, and Ostwald ripening suppression are common ways surfactants can influence crystallite size[27,28,32,33]. According to Mastuli et al.[27], the shape of the crystal changes due to the precursor particles becoming stuck inside the CTAB micelles throughout the sol-gel process. The micelles were eliminated after calcination, resulting in MgO taking on the spherical shape. It aligns well with the TGA profile when the prominent decomposition peak shifted to a higher temperature.

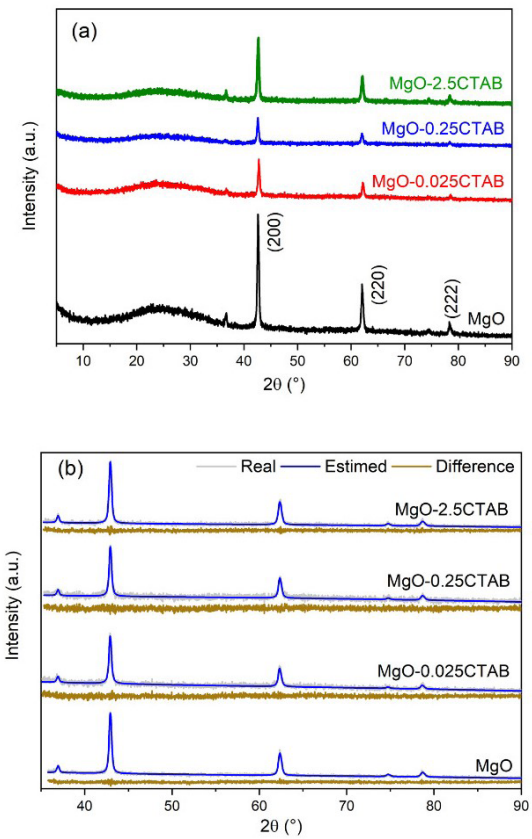

Figure 2. (a) XRD diffraction patterns of the parent magnesium oxide (MgO) and the sol-gel samples using CTAB and (b) plots from structural refinement from Rietveld analysis.

Table 1. Crystallographic parameters obtained by the Rietveld refinement of the XRD patterns.

Sample	Cell parameter (Å)	Cryst. Size (Å)	Microstrain ξ (x10^{-3})	O occupancy	R_{wp} (%)
MgO	4.2097± 0.0005	53.8 ± 0.1	1.1	0.94	9.0
MgO-0.025CTAB	4.2114 ± 0.0011	47.1 ± 0.2	0.4	0.82	12.3
MgO-0.25CTAB	4.2099 ± 0.0012	51.1 ± 0.2	0.8	0.83	13.8
MgO-2.5CTAB	4.2103 ± 0.0007	52.5 ± 0.1	1.2	0.88	12.4

There was a decrease in crystallite size with the MgO-0.025CTAB sample and successive increases after that. This behavior may be related to the excess of CTAB when the interaction among CTAB molecules was preferred to the magnesium species[28,33]. The behavior is maintained up to the maximum CTAB concentration in the MgO-2.5CTAB sample.

Microstrain (ξ) in crystallites refers to the local strain or distortions within the crystal structure, and it is often influenced by factors such as defects, dislocations, and lattice imperfections[34]. There was a decrease in the microstrain for MgO-0.025CTAB and MgO-0.25CTAB, possibly related to magnesium species and CTAB association. The microstrain returned to MgO level in MgO-2.5CTAB, suggesting a non-effective interaction between the surfactant and the magnesium species. Despite the microstrain behavior, the oxygen occupancy decreases, suggesting more oxygen vacancy in the structure of CTAB prepared samples.

The N_2 adsorption/desorption isotherms are illustrated in Figure 3a, and the textural properties are presented in Table 2. The isotherm profile for the MgO sample is of type II, according to the classification of IUPAC[35], which is indicative of the absence of pores (2 m^2/g). The same profile of isotherm was found in MgO-0.025CTAB and MgO-0.25CTAB samples. Compared to MgO, the lower nitrogen adsorption after 0.95 p/p_0 indicates more aggregated particles, probably due to the interaction of the CTAB species on the surface. For the MgO-0.025CTAB and MgO-0.25CTAB, the specific area was 9 and 20 m^2/g, respectively. However, for the MgO-2.5CTAB sample, the isotherm was slightly different from the other samples. There was a considerable increase in N_2 adsorption and the formation of a small hysteresis, which may be related to forming a pore system. Still, the absence of a plateau near $p/p_0 = 1$ indicates the existence of macropores (diameter > 50 nm). The pore distribution (Figure 3b) clearly shows the increase of pores after 50 nm for MgO-2.5CTAB. The surfactant introduction during the synthesis increases the specific area by creating pores in the mesoporous and macroporous regions. The CTAB surfactant is regularly utilized as an amphiphilic template because of its tall atomic weight (5800 g/mol), which produces moderately huge mesopores and thick inorganic dividers, conferring more stability to the material, compared to the utilization of moo atomic weight surfactants. Besides, its utilization leads to an alteration within the crystallite estimate, as confirmed by XRD[2,36,37]. Therefore, the CTAB acts as a dispersant and a structure-directing.

The scanning electron micrographs of samples MgO, MgO-0.025CTAB, MgO-0.25CTAB, and MgO-2.5CTAB (Figure 4) reveal the overall size and morphology of the outer surface of the crystals are affected by CTAB presence. This corroborates with the data obtained by XRD, indicating that a higher concentration of CTAB (Figure 4b) seemed similar to the MgO sample (Figure 4a). Initially, MgO consists of nonuniform shape aggregate that can justify the amorphous contribution on XRD pattern. The MgO surface showed a smooth roughness, similar to MgO-2.5CTAB. On the other hand, with the decrease in CTAB concentration, the surface appeared to be increasingly rougher, as in the MgO-0.025CTAB sample (Figure 4d). These results are also in line with XRD results with microstrains.

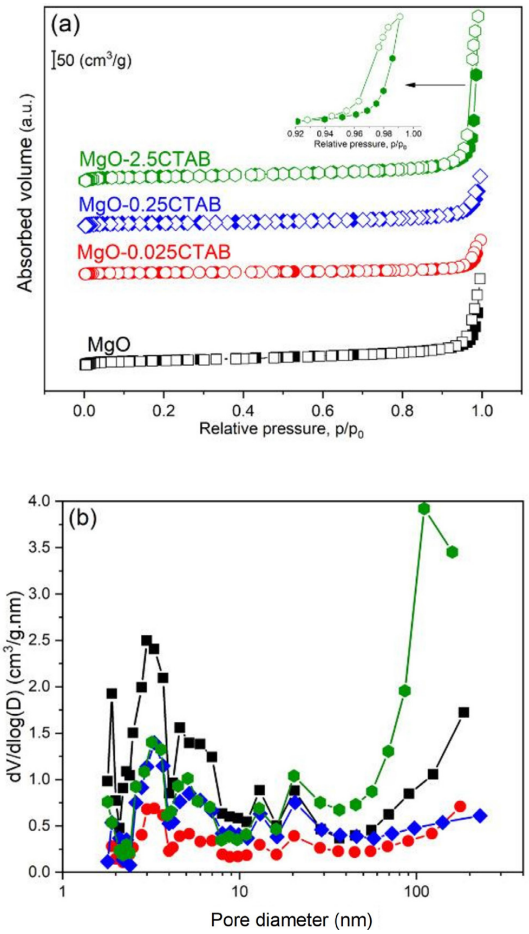

Figure 3. (a) Nitrogen adsorption-desorption isotherms (filled points correspond to nitrogen adsorption and empty points to desorption), (b) BJH pore size distribution based on desorption branch of the isotherms of MgO, MgO-0.025CTAB, MgO-0.25CTAB, MgO-2.5CTAB.

Table 2. Textural properties of the samples.

Sample	S_{BET} (m^2/g)	Vol. (cm^3/g)	Average mesopore size (nm)
MgO	32	0.0042	4.9
MgO-0.025CTAB	9	0.0011	4.8
MgO-0.25CTAB	20	0.0021	4.1
MgO-2.5CTAB	25	0.0016	2.4

Figure 5 shows the size distribution of the crystals. The MgO had an average size of 19.1 µm. Given the relative size distribution, contributions between 20 and 25 µm had a relevant weight. There was no detection of crystals smaller than 10 µm. On the other hand, the MgO-0.025CTAB sample has a contribution below 10 µm and an average size of 17.3 µm.

Furthermore, the most significant weight in the relative distribution ranges between 10 and 15 µm was found in MgO-0.25CTAB. These results align with the average crystallite size found by refining the parameters using the Rietveld method. MgO-0.25CTAB and MgO-2.5CTAB also showed crystals below 10 µm, showing that CTAB was decisive for forming smaller crystals. The average sizes were 18.8 and 17.3 µm for MgO-0.25CTAB and MgO-2.5CTAB, respectively.

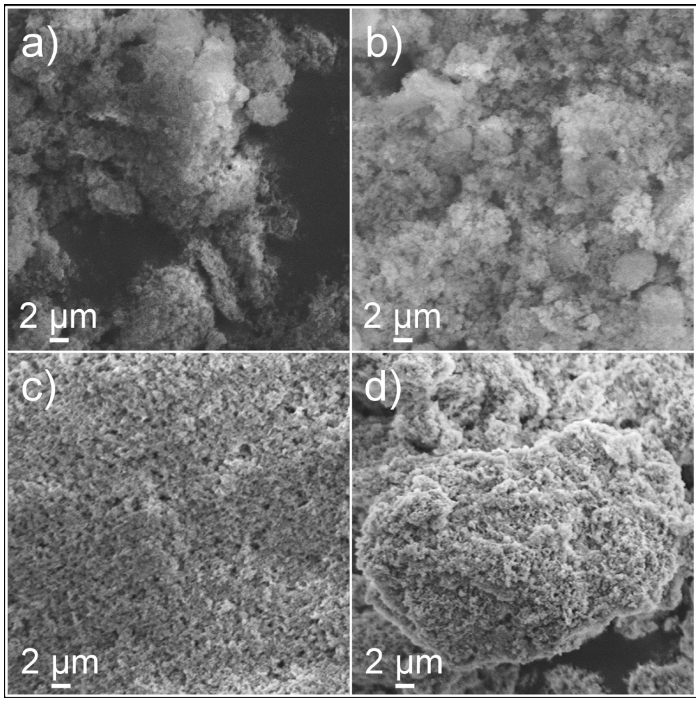

Figure 4. Scanning electron micrographs at magnifications of 2,000x for (a) MgO, (b) MgO-2.5CTAB, (c) MgO-0.25CTAB, and (d) MgO-0.025CTAB.

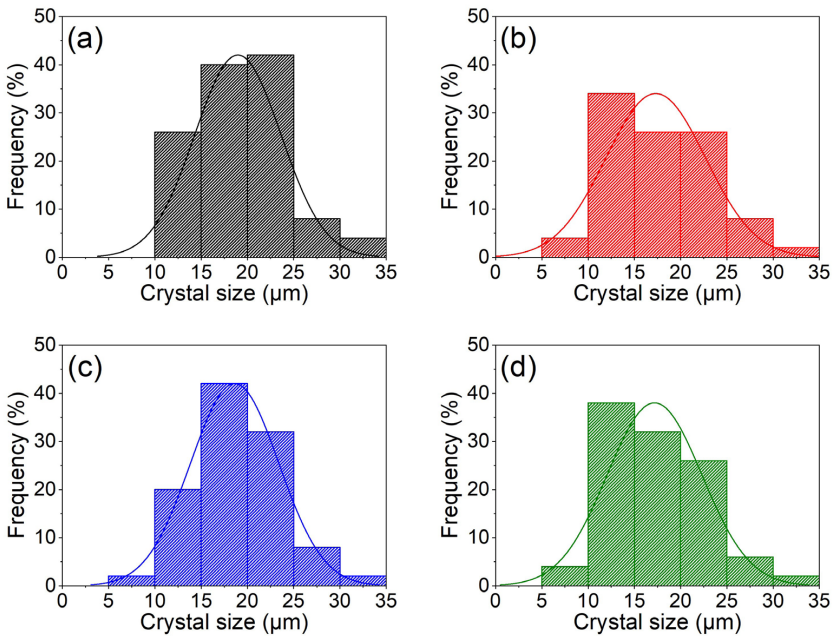

Figure 5. Crystal size distribution obtained from SEM micrographs for (a) MgO, (b) MgO-0.025CTAB, (c) MgO-0.25CTAB, and (d) MgO-2.5CTAB.

The set of results presented made it possible to structure a scheme (Figure 6) that presents the relationship between the structure formed and the concentration of CTAB used in the synthesis. The surfactant allowed smaller crystals to be present in the MgO-0.025CTAB sample compared to MgO. An increase of 10x contributed to this sense in MgO-0.25CTAB. However, with a significant excess of CTAB in the MgO-2.5CTAB sample, part of it interacts with the CTAB molecules themselves, leaving part of the magnesium species isolated, approaching the result of the MgO sample without CTAB[28].

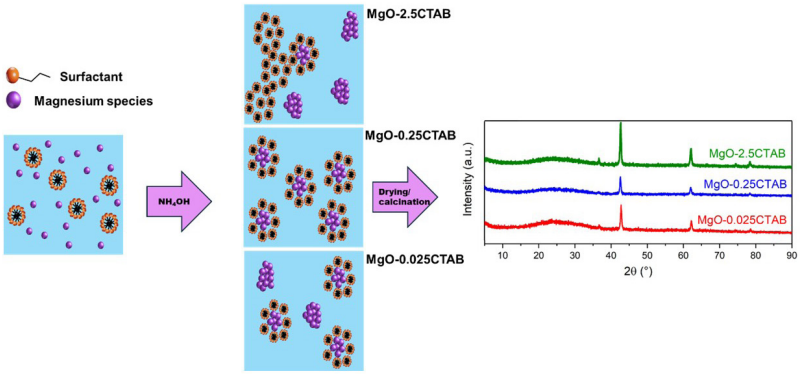

Figure 6. Scheme of CTAB and magnesium species as a function of CTAB concentration.

4. Conclusions

According to the TGA data, it is possible to observe the interaction between CTAB and magnesium species by the shift to higher decomposition temperature from 360 to 400 ºC for MgO-0.025CTAB and MgO-0.25CTAB samples. The excess of CTAB revealed a TGA profile similar to pure CTAB surfactant in MgO-2.5CTAB, suggesting an isolated organic system. With the X-ray diffraction patterns, it was possible to observe a decrease in the signal of the main peaks with CTAB introduction. However, the tendency to an isolated organic/inorganic system was confirmed in MgO-2.5CTAB by increasing the reflection peak intensity.

The Rietveld refinement shows that microdeformations decrease with CTAB introduction, suggesting an organization promoted by the surfactant, except MgO-2.5CTAB sample, in agreement with previous results. The physisorption of N_2 showed that the samples presented a type II isotherms, showing the absence of pores (2 m^2/g), and with scanning electron microscopy it was possible to observe that the introduction of CTAB did not present changes in the MgO crystals that did not present a defined structure, only showing a slight increase in the surface roughness of the samples.

5. Acknowledgments

The São Paulo State Research Foundation (FAPESP, grants #2023/03909-1, #2023/04143-2, #2021/05246-4, and #2021/02152-9) and CAPES (024/2012 Pro-equipment and 011/2009) provided financial support for this work.

6. References

1. Li Z, Chen J, Xie Y, Wen J, Weng H, Wang M, et al. Zonal activation of molecular carbon dioxide and hydrogen over dual sites Ni-Co-MgO catalyst for CO_2 methanation: synergistic catalysis of Ni and Co species. Journal of Energy Chemistry. 2024;91:213-25.
2. Possato LG, Gonçalves RGL, Santos RMM, Chaves TF, Briois V, Pulcinelli SH, et al. Sol-gel synthesis of nanocrystalline MgO and its application as support in Ni/MgO catalysts for ethanol steam reforming. Appl Surf Sci. 2021;542:148744.
3. Liu H, Huang W, Yu Z, Wang X, Jia Y, Huang M, et al. High-performance CuMgAl catalysts derived from hydrotalcite for CO_2 hydrogenation to methanol: effects of Cu-MgO interaction. Mol Catal. 2024;558:114002.
4. Owens GJ, Singh RK, Foroutan F, Alqaysi M, Han CM, Mahapatra C, et al. Sol-gel based materials for biomedical applications. Prog Mater Sci. 2016;77:1-79.
5. Hernández Ortiz GM, Parra R, Fraile-Sainz J, Domingo C, Fanovich MA. Porous hydroxyapatite-titanium dioxide composites prepared by a sol-gel / supercritical CO_2-drying combined process. Ceram Int. 2024;50(8):13298-307.
6. Villarreal-Lucio DS, Rivera Armenta JL, Estrada Moreno IA, Garcia-Alamilla R. Effect of surfactant in particle shape and thermal degradation of eggshell particles. Mater Res. 2019;22(3):e20180778.
7. Possato LG, Pereira E, Gonçalves RGL, Pulcinelli SH, Martins L, Santilli CV. Controlling the porosity and crystallinity of MgO catalysts by addition of surfactant in the sol-gel synthesis. Catal Today. 2020;344:52-8.
8. Modak A, Bhanja P, Dutta S, Chowdhury B, Bhaumik A. Catalytic reduction of CO_2 into fuels and fine chemicals. Green Chem. 2020;22(13):4002-33.
9. Al-Mamoori A, Krishnamurthy A, Rownaghi AA, Rezaei F. Carbon capture and utilization update. Energy Technol. 2017;5(6):834-49.
10. Zhang Z, Pan SY, Li H, Cai J, Olabi AG, Anthony EJ, et al. Recent advances in carbon dioxide utilization. Renew Sustain Energy Rev. 2020;125:109799.
11. Medford AJ, Vojvodic A, Hummelshøj JS, Voss J, Abild-Pedersen F, Studt F, et al. From the Sabatier principle to a predictive theory of transition-metal heterogeneous catalysis. J Catal. 2015;328:36-42.
12. Trimm DL. Catalysts for the control of coking during steam reforming. Catal Today. 1999;49(1-3):3-10.
13. Zanganeh R, Rezaei M, Zamaniyan A. Dry reforming of methane to synthesis gas on NiO-MgO nanocrystalline solid solution catalysts. Int J Hydrogen Energy. 2013;38(7):3012-8.
14. Meshkani F, Rezaei M. Nickel catalyst supported on magnesium oxide with high surface area and plate-like shape: a highly stable and active catalyst in methane reforming with carbon dioxide. Catal Commun. 2011;12(11):1046-50.
15. Manjunatha KG, Swamy BEK, Madhuchandra HD, Gururaj KJ, Vishnumurthy KA. Synthesis and characterization of MgO nanoparticle and their surfactant modified carbon paste electrode sensing for paracetamol. Sensors International. 2021;2:100127.
16. Climent MJ, Corma A, Iborra S, Mifsud M. MgO nanoparticle-based multifunctional catalysts in the cascade reaction allows the green synthesis of anti-inflammatory agents. J Catal. 2007;247(2):223-30.
17. Danks AE, Hall SR, Schnepp Z. The evolution of "sol-gel" chemistry as a technique for materials synthesis. Mater Horiz. 2016;3(2):91-112.

18. Hench LL, West JK. The sol-gel process. Chem Rev. 1990;90(1):33-72.
19. Roggenbuck J, Tiemann M. Ordered mesoporous magnesium oxide with high thermal stability synthesized by exotemplating using CMK-3 carbon. J Am Chem Soc. 2005;127(4):1096-7.
20. Tian P, Han XY, Ning GL, Fang HX, Ye JW, Gong WT, et al. Synthesis of porous hierarchical MgO and its superb adsorption properties. ACS Appl Mater Interfaces. 2013;5(23):12411-8.
21. Hanif A, Dasgupta S, Nanoti A. Facile synthesis of high-surface-area mesoporous MgO with excellent high-temperature CO_2 adsorption potential. Ind Eng Chem Res. 2016;55(29):8070-8.
22. Rietveld HM. A profile refinement method for nuclear and magnetic structures. J Appl Cryst. 1969;2:65-71.
23. Lutterotti L. Maud: a Rietveld analysis program designed for the internet and experiment integration. Acta Crystallogr A. 2000;56(S1):S54.
24. Brunauer S, Emmett PH, Teller E. Adsorption of gases in multimolecular layers. J Am Chem Soc. 1938;60(2):309-19.
25. Barrett EP, Joyner LG, Halenda PP. The determination of pore volume and area distributions in porous substances. I. Computations from nitrogen isotherms. J Am Chem Soc. 1951;73(1):373-80.
26. Pei L-Z, Yin W-Y, Wang J-F, Chen J, Fan C-G, Zhang Q-F. Low temperature synthesis of magnesium oxide and spinel powders by a sol-gel process. Mater Res. 2010;13(3):339-43.
27. Mastuli MS, Ansari NS, Nawawi MA, Mahat AM. Effects of cationic surfactant in sol-gel synthesis of nano sized magnesium oxide. APCBEE Procedia. 2012;3:93-8.
28. Piperopoulos E, Mastronardo E, Fazio M, Lanza M, Galvagno S, Milone C. Enhancing the volumetric heat storage capacity of $Mg(OH)_2$ by the addition of a cationic surfactant during its synthesis. Appl Energy. 2018;215:512-22.
29. Gerlach W, Stern O. Das magnetische moment des silberatoms. Z Physik. 1922;9:353-5.
30. Mukherjee P, Padhan SK, Dash S, Patel S, Mishra BK. Clouding behaviour in surfactant systems. Adv Colloid Interface Sci. 2011;162(1-2):59-79.
31. Bakshi MS. How surfactants control crystal growth of nanomaterials. Cryst Growth Des. 2016;16(2):1104-33.
32. Prado DC, Fernández I, Rodríguez-Páez JE. MgO nanostructures: synthesis, characterization and tentative mechanisms of nanoparticles formation. Nano-Struct Nano-Objects. 2020;23:100482.
33. Díez R, Medina OE, Giraldo LJ, Cortés FB, Franco CA. Development of nanofluids for the inhibition of formation damage caused by fines migration: effect of the interaction of quaternary amine (CTAB) and MGO nanoparticles. Nanomaterials. 2020;10(5):928.
34. Sotomayor F, Quantatec AP, Sotomayor FJ, Cychosz KA, Thommes M. Characterization of micro/mesoporous materials by physisorption: concepts and case studies. Acc Mater Surf Res. 2018;3(2):34-50.
35. Qin W, Nagase T, Umakoshi Y, Szpunar JA. Relationship between microstrain and lattice parameter change in nanocrystalline materials. Philos Mag Lett. 2008;88(3):169-79.
36. Rezaei M, Khajenoori M, Nematollahi B. Preparation of nanocrystalline MgO by surfactant assisted precipitation method. Mater Res Bull. 2011;46(10):1632-7.
37. Possato LG, Pulcinelli SH, Martins L, Briois V, Santilli CV. Appraisal of Ni species supported on porous MgO during ethanol steam reforming by XAS. ChemCatChem. 2022;14(21):e202200684.

Supplementary material

The following online material is available for this article:

Figure S1 - TGA pattern of CTAB compound.